# INVESTIGATION OF A HIPPED PLATE ROOF STRUCTURE

by

JAI BIN KIM

A THESIS

submitted to

OREGON STATE COLLEGE

in partial fulfillment of
the requirements for the
degree of

MASTER OF SCIENCE

June 1960

APPROVED:

_____

Professor of Civil Engineering

       In Charge of Major

_____

Head of Department of Civil Engineering

_____

Chairman of School Graduate Committee

_____

Dean of Graduate School

Date thesis is presented _May 2, 1960_

Typed by Judith Bechtel

## ACKNOWLEDGEMENT

Acknowledgement is due Thomas J. McClellan, Professor of Civil Engineering, for the original idea of this thesis and for his contributions to it. The writer would also like to express his appreciation to Professor Glenn W. Holcomb, Head of the Civil Engineering Department, for his support and advice on this project.

# TABLE OF CONTENTS

# TABLE OF CONTENTS - Continued

# INVESTIGATION OF A HIPPED PLATE ROOF STRUCTURE

## PART I

### INTRODUCTION

Folded plate thin shells for roofs of large buildings are defined as structures in which the loads are sustained by thin folded flat plates. These folded plate structures, or as they are sometimes called, prismatic shells or hipped plates, have an economic and aesthetic advantage over certain other methods of roofing large buildings. This type has an advantage over thin curved shells in that it is easier to form, fabricate and design.

This paper deals with a "three-segment (horizontal projection)" plywood hipped plate roof simply supported by two end diaphragms. Although this type of structure takes advantage of the effective use of the monolithic properties of the material such as reinforced concrete, the writer attempted to extend both theoretical and experimental investigations to the plywood structure which is not homogeneous, nor monolithic.

The first folded plate structure was constructed in Germany in 1925 for use as coal bunkers where the ratio of the span length to the width of plate is large.

G. Ehlers and H. Craemer published the first design
theory in 1930, in which the rigidity of the joints was
entirely neglected. In 1932 E. Gruber published a paper
in which he considered the effect of the rigidity of the
joints, the connecting moments along the common edges of
the plates, and the effect of the relative displacements
between the joints (4, p. 744). The practice of this
type of roof started in America as early as 1935 when
L. H. Nishkan designed and built a warehouse in San
Francisco using hipped plate theory. Since then, however,
the folded plate construction had been ignored preceding
World War II. After the War many investigations have
been conducted. Interest in this type of roof has
increased considerably since the first paper on the design
theory was published in this country by Winter and Pei in
1947. They adopted the method of analysis in the European
countries to the American practice and developed a distri-
bution method (11, p. 506). Among many investigations,
the most valuable contribution to this field was done by
I. Gaafar in 1954. Gaafar did both theoretical and
experimental work on an aluminum model of a three-segment
hipped plate roof. In his analysis, Gaafar included joint

displacements as well as previous fundamental hipped plate
theories.  It was not new to consider the joint displace-
ments, but Gaafar simplified it tremendously.  However,
he neglected the fact that the longitudinal edges of
plates are on the elastic supports, such that a part of
the uniformly distributed load in longitudinal direction
is translated transversely by the slab action due to the
displacement along the longitudinal edges of the plate.
In a relaxation method for the corrected longitudinal
stresses, it is more accurate and simpler to solve simul-
taneous equations than to use a moment distribution method.

In designing the folded plate, the longitudinal
bending of a plate (out of its plane) takes an important
role in addition to the transverse slab action and longi-
tudinal plate action.  This was witnessed by the
difference in the longitudinal strain gage readings
between inner and outer surface of the model, especially
in the edge beam.  This type of bending would be a
critical factor in designing reinforced concrete hipped
plate structures.

# PART II

## THEORY

A.  Ordinary Beam Approach

Assuming no relative displacement of joint and no relative rotations between the adjacent plates, the structure is treated as a box beam.  In this type of approach the loads are sustained by the beams at all joints along the edges of the plate.

B.  Assumptions Made in Analyzing the Simply Supported Hipped Plate Structure

1.  The material is uniform and elastic.

2.  The cross section of the plate is rectangular shape.

3.  All joints are rigid and torsional resistances or effects on the plate are neglected.

4.  Stresses vary linearly across the width of each plate.

5.  The ratio of length to the width of the plate is large, such that the plate can be treated as a one-way slab.

## C.   Hipped Plate Theory

Since a part of the surface load is transmitted to the longitudinal edges of the plate, because of the difficulty in expressing such a loading condition, the corrective surface load can be approximated by the sum of partial loads which produces the sinusoidal elastic line for a simply supported roof structure.  This complies with the previous assumptions in which the elastic line of a beam carrying uniform or concentrated load is a half sine wave.  The intensity of the sum of partial load is defined as $An \sin \frac{n\pi x}{l}$ , in which n is any integer.  This trigonometric function is defined as a series of the form

$$\frac{a_0}{2} + a_1 \cos \frac{\pi x}{l} + a_2 \cos \frac{2\pi x}{l} + \cdots \cdot a_n \cos \frac{n\pi x}{l}$$

$$+ b_1 \sin \frac{\pi x}{l} + b_2 \sin \frac{2\pi x}{l} + \cdots \cdot b_n \sin \frac{n\pi x}{l} \, .$$

Expand this trigonometric function defined by the relations,
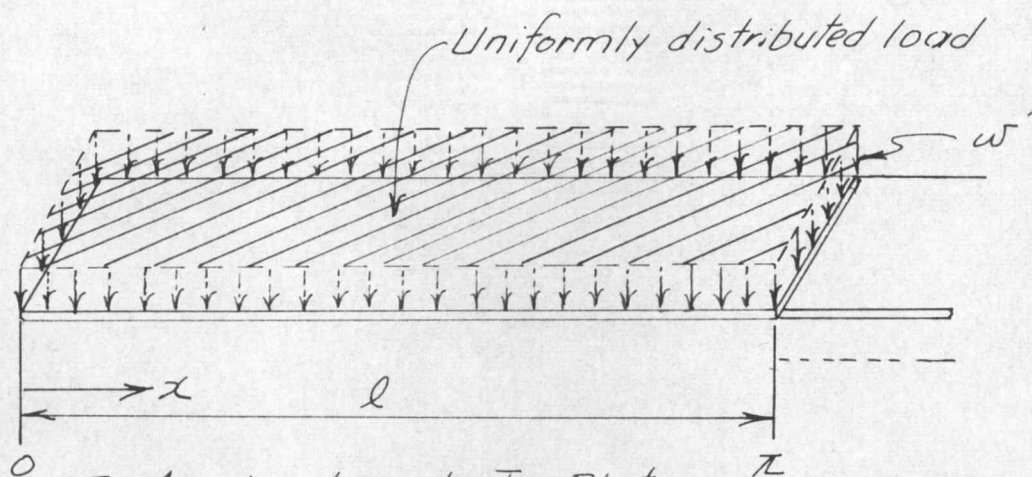
Fig. 1 — Load on the Top Plate

$$f(x) = w', \qquad 0 < x < \pi \text{ or } l,$$

$$f(x) = -w', \qquad l \text{ or } \pi < x < 2\pi \text{ or } 2l,$$

in Fourier series.

From the Fourier formulas (5, p. 138),

$$a_0 = \frac{1}{\pi} \int_c^{c+2\pi} f(x)\, dx = \frac{1}{\pi} \int_0^{2\pi} f(x)\, dx = \frac{1}{\pi} \int_0^{2l} f(x)\, dx = 0$$

$$a_n = \frac{1}{\pi} \int_0^{2\pi} f(x) \cos \frac{n\pi x}{l}\, dx = 0$$

$$b_n = \frac{1}{\pi} \int_0^{2\pi} f(x) \sin \frac{n\pi x}{l}\, dx = \frac{1}{\pi} \int_0^{\pi} w' \sin \frac{n\pi x}{l}\, dx$$

$$+ \frac{1}{\pi} \int_0^{2\pi} (-w') \sin \frac{n\pi x}{l}\, dx = \frac{2w'}{n\pi} [1 - \cos n\pi]$$

$$f(x) = p = \sum_{n=1}^{\infty} b_n \sin \frac{n\pi x}{\ell}$$

$$= \frac{4\omega'}{\pi} \left[ \sin \frac{\pi x}{\ell} + \frac{1}{3} \sin \frac{3\pi x}{\ell} + \cdots\cdots \right]$$

$$= \frac{4\omega'}{\pi} \sum_{n=1,3,5,\ldots} \frac{1}{n} \sin \frac{n\pi x}{\ell} \qquad\qquad\text{(1)}$$

For simplicity and sufficient accuracy for preliminary design purpose, the first term of Eq. (1) is used. Line load along the longitudinal direction, then, is

$$P = \frac{4\omega'}{\pi} \sin \frac{\pi x}{\ell} \qquad\qquad\text{(1')}$$

Load in the transverse direction varies uniformly. The sections, transversely cut as a continuous one-way slab supported by imaginary reactions at the joints of the longitudinal plates, are analyzed. Analyzing a continuous one-way slab, any type of loads can be transformed into the loads acting at the joints. These joint loads are resolved into two components parallel to the two adjacent plates. The components of the joint loads cause the independent bending in each plate which acts as a deep beam simply supported by end diaphragms. Unequal longitudinal edge stresses at the joints do not comply with the continuity requirements. Consequently, the shear stresses are bound to act along the common edges in order to prevent

the relative movements of the adjacent plates. Creating the imaginary two equal and opposite forces at the common edges, the corrected longitudinal stresses are found.

The relative displacement of joints are derived from the plate deflections which cause the plate to rotate. Again analyzing a continuous one-way slab, plate loads are found. Then the process for unyielding supports is repeated. The longitudinal plate stresses (out of plane) are found by using the deflection perpendicular to the plate.

D.  Analytical Criteria for Design

Stresses to be found for designing the hipped plate roof structure are divided into three stages:

1.  the longitudinal stresses.

2.  the transverse stresses.

3.  the longitudinal (out of plane) stresses.

# PART III

# DESIGN OF A PLYWOOD MODEL

## A.  Material Descriptions

Douglas fir plywood sanded 1/2 inch thick, of five layers, is used with the face plies running parallel to longitudinal direction, in accordance with the specification provided by the Douglas Fir Plywood Association.

When plywood is subject to a tensile or compressive force parallel to its length, only those plies having their grains running parallel to its length are considered as contributing to load carrying capacity. The cross plies are stressed across the grain and thus are incapable of contributing any significant amount to the strength of plywood in tension or compression. Similarly, in flexure, only the plies running parallel to the span are considered in computing the moment of inertia of the cross section (3, Section Two, p. 1).

Neglecting the moment of inertia of the face plies when plywood is used in flexure with its face grain perpendicular to the span,

$$I_\perp = \frac{1}{12}\left[ \left(\frac{11}{32}\right)^3 - \left(\frac{3}{32}\right)^3 \right] = 0.00333 \ in^4$$

**B.   Ordinary Beam Approach**

For a total load of 792 pounds uniformly distributed over the plate CC',
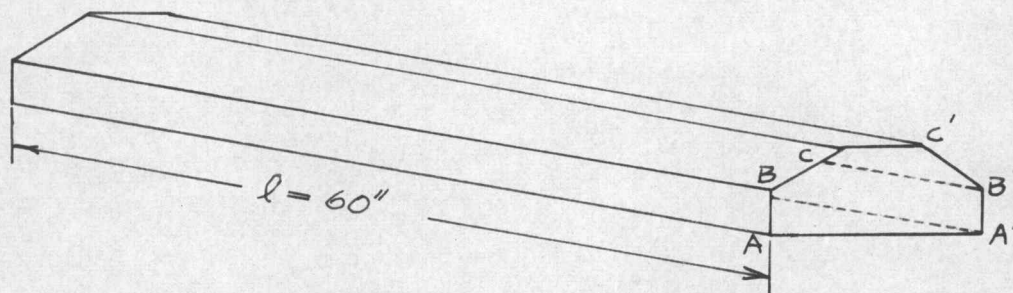


Fig. 2 — Hipped plate Roof
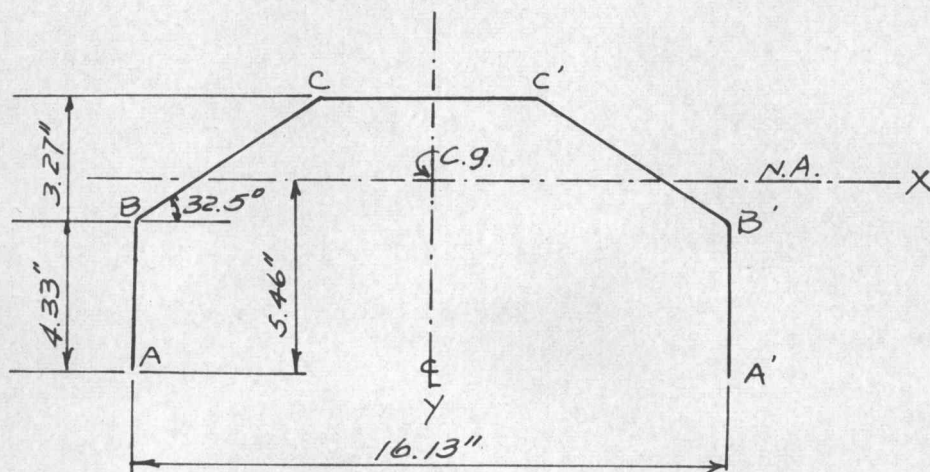


Fig. 3 — Cross Section of Roof

$$I_{xx} = 37.32 \ in^4$$

$$w, \ load/linear \ inch, = 792/60 = 13.2 \ lbs/in$$

$$\text{Maximum Moment} = \frac{\omega \ell^2}{8} = 5,930 \ lb\text{-}in$$

Maximum Unit Stresses on Top Fiber,

$$= -\frac{M_{max} C}{I_{xx}}$$

$$= -\frac{(5,930)(2.14)}{37.32}$$

$$= -340 \ psi$$

Maximum Unit Stresses on Bottom Fiber,

$$= +\frac{(340)(5.46)}{2.14}$$

$$= +867 \ psi$$

Maximum Unit Stresses on the Top of the Edge Beam,

$$= +\frac{(340)(1.13)}{2.14}$$

$$= +180 \ psi$$

There is no doubt that the applicability of ordinary beam approach for this hipped plate model is doubtful

because of the lack of complete rigidity of the joint, the bending (out of plane) of the edge beam, and in part the nonhomogeneity of the material.

C.  Theoretical Analysis by Hipped Plate Theory

The brief design procedure for the symmetrical and simply supported hipped plate structure is as follows:

1. Assume that the joints of the plates are held by the unyielding elastic supports.

2. Cut one inch center strip transversely and treat this strip to act as a continuous one-way slab.

3. Compute the transverse moments at the joints which cause the joint loads. Total joint loads are found by adding the joint loads by transverse moment to the joint loads by the applied load on the plate.

4. Resolve these joints loads into two components parallel to the adjacent plates to get the plate loads. Compute the longitudinal plate stresses.

5. Correct the longitudinal plate stresses found in Step 4. This correction is provided by the

requirement for compatible stresses in two
adjacent plates at their common edge.

6. Assuming that the outer edge plate can rotate
   freely, compute the transverse moments due to
   the plate rotations. Repeat the Steps 3 to 5
   to get the longitudinal stresses.

7. Final longitudinal plate stresses are found by
   adding the longitudinal plate stresses by Step 5
   and by Step 6.

8. Transverse moments are superimposed similarly as
   in Step 7.

9. Compute the deflections perpendicular to the
   plates.

10. Using deflections found in Step 9. Compute the
    longitudinal stresses (out of plane) at edges.

The hipped plate roof shown in Fig. 4 will be analyzed.
A total load of 792 pounds is placed on the top plate only.
Neglecting the dead load, $w' = 792/(60)(6) = 2.2 \ lb/in^2$
is assumed as live load.

symmetrical about ₵
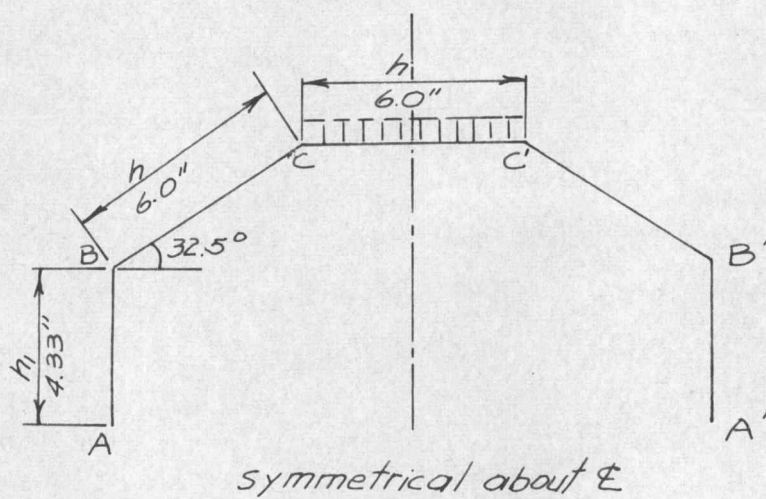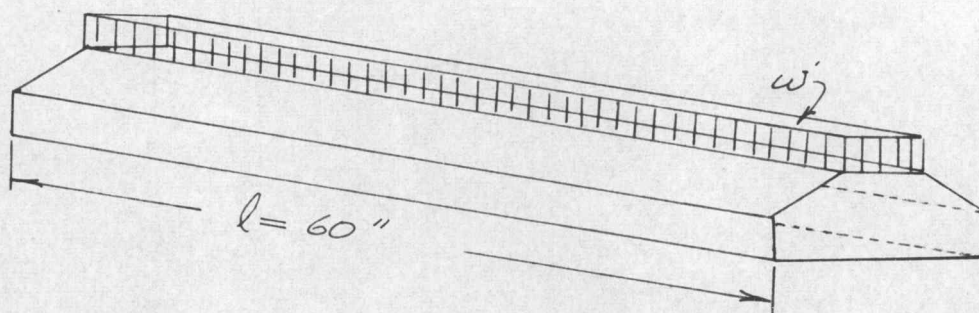
Fig. 4 — Proposed Plywood Model

D.  Case I.

Assuming the Unyielding Elastic Support of A Continuous Ony-way Slab (transverse)

For 1 inch center strip.

$$P_o, \text{ line load, } \frac{lb}{in/in} = \frac{4W'}{\pi} \sin \frac{\pi \frac{\ell}{2}}{\ell} = \frac{4W'}{\pi}$$
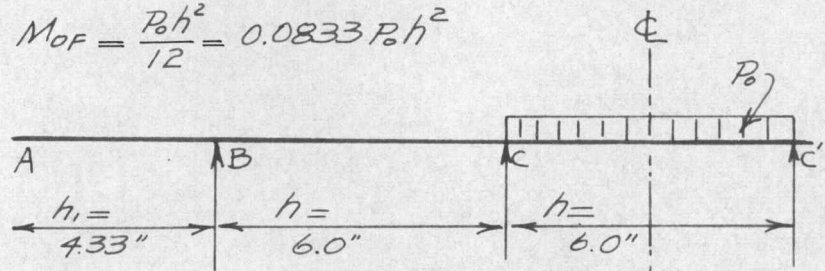
$$M_{OF} = \frac{P_o h^2}{12} = 0.0833 \, P_o h^2$$



| | $h_1 = 4.33''$ | | $h = 6.0''$ | | $h = 6.0''$ | |

Relative $k$     ①     ①

Adjusted $k$     ③⁄₄     ½

F E M

$$-0.0833 P_o h^2 \qquad +0.0833 P_o h^2$$

$$+0.05 P_o h^2 \quad +0.0333 P_o h^2 \quad -0.033 P_o h^2$$

Moment

$$+0.05 P_o h^2 \quad -0.05 P_o h^2$$

Shear

$0.05 P_o h \qquad 0.05 P_o h \quad 0.5 P_o h \qquad 0.5 P_o h$
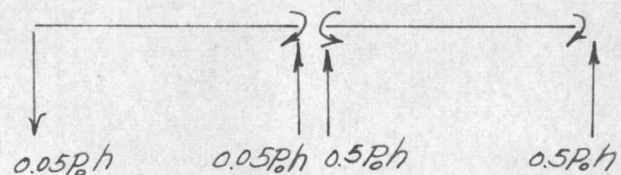
Fig. 5 — Transverse Moment and Shear
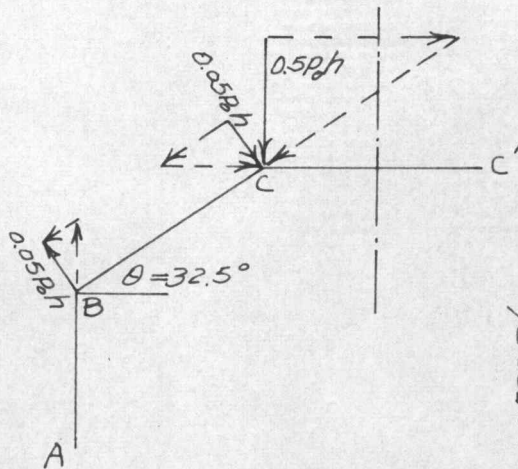
Fig. 6 — Joint Loads and
Its Components
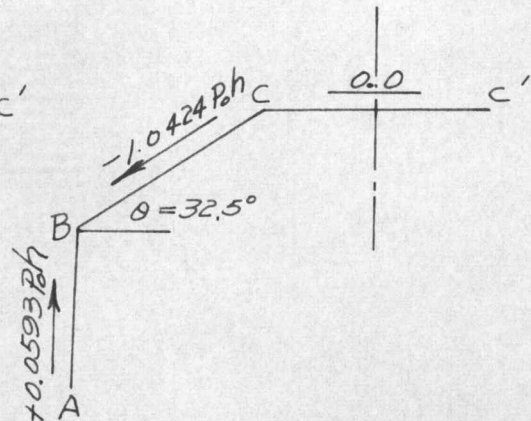
Fig. 7 — $Q_0$, Plate Loads

Sign convention : Clockwise direction is positive,
and tension is positive.

Since plate loads vary as a half sine wave
longitudinally, namely $Q = Q_0 \sin \frac{\pi x}{\ell}$,

the longitudinal moment, $M$

$$= \frac{\ell^2}{\pi^2} Q_0 \sin \frac{\pi x}{\ell}$$

$$M_0 = \frac{\ell^2}{\pi^2} Q_0$$

$$M_{0AB} = \left(\frac{\ell^2}{\pi^2}\right)(-1.0424 \, P_0 h)$$

$$M_{0BC} = \left(\frac{\ell^2}{\pi^2}\right)(0.0593 P_0 h)$$



Fig. 8 — $Q = Q_0 \sin \frac{\pi x}{\ell}$
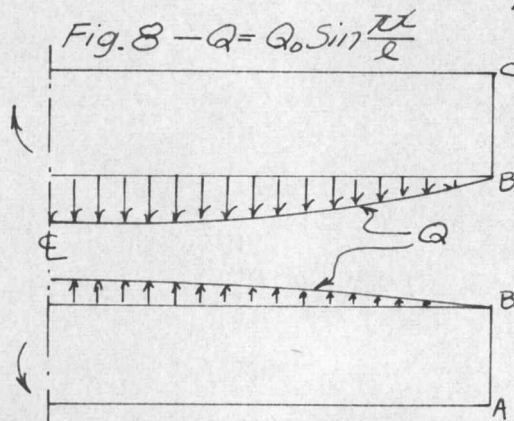
| Plate | $M_0$ , lb-in | Section Modulus, $Z$, in$^3$ | Stresses, psi |
|-------|----------------|------------------------------|----------------|
| AB | $(\ell/\pi)^2 (0.0593 P_0 h)$ | $Z = 0.782$ | $\pm f_1 = 465$ |
| BC | $(\ell/\pi)^2 (-1.0424 P_0 h)$ | $Z = 1.5$ | $\pm f_2 = 4{,}260$ |
| CC' | $0$ | $Z = 1.5$ | $0$ |

TABLE 1 — Computation of the Longitudinal Stresses
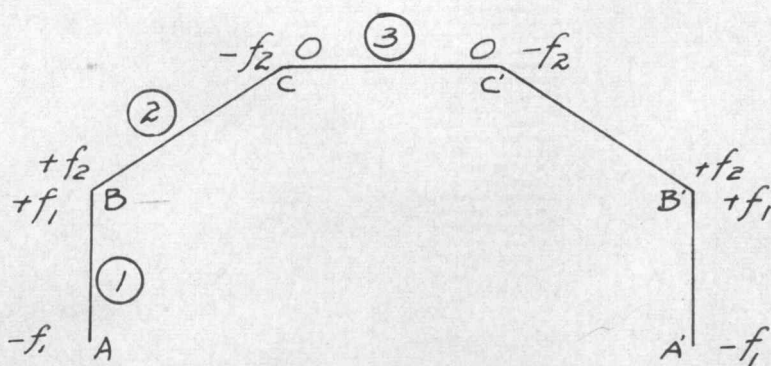
Fig. 9 —Longitudinal Edge Stresses

Due to unbalanced longitudinal edge stresses, longitudinal sliding would occur at the joint of two adjacent plates. In order to prevent this sliding, two equal opposite forces are introduced to produce the longitudinal edge shears. Directions of these opposite forces are determined according to the magnitude of each edge stress.
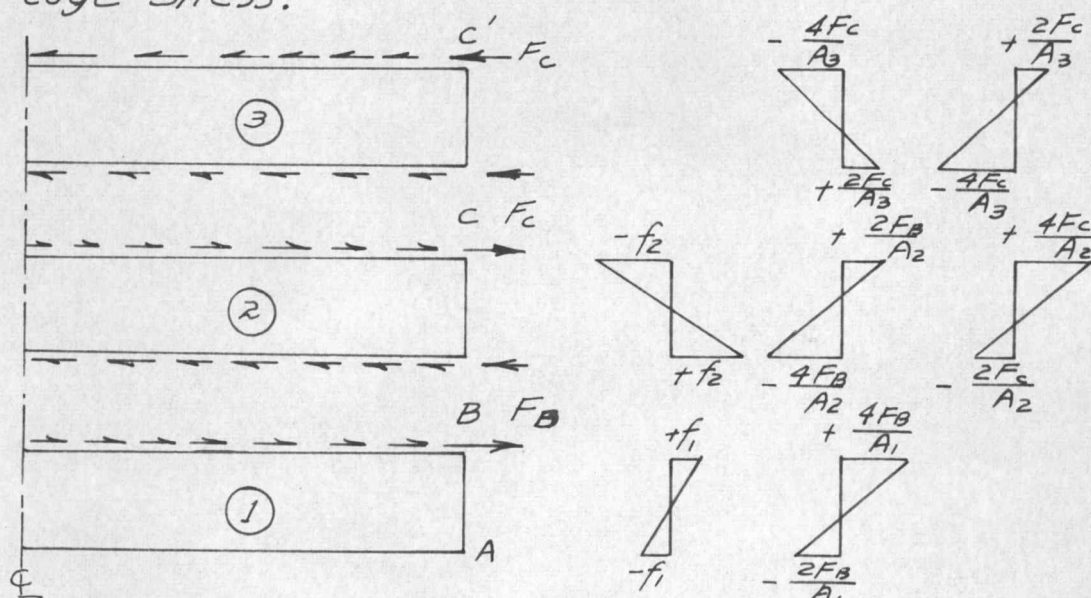


Fig. 10 —Edge Stresses by Edge Forces

Since the edge stresses are equal along the joint of two adjoining plates,

at joint C

$$\frac{4F_c}{A_2} + \frac{2F_B}{A_2} - f_2 = -\frac{2F_c}{A_3} \qquad (2)$$

at joint B

$$-\frac{2F_c}{A_2} - \frac{4F_B}{A_2} + f_2 = \frac{4F_B}{A_1} + f_1 \qquad (3)$$

Solving Eqs.(2) and (3),

$$F_c = \frac{t(26f_1 + 98f_2)}{115.3}$$

$$F_B = \frac{tf_2(3)(115.3) - 3t(26f_1 + 98f_2)}{115.3}$$

Substituting the values of $F_c$ and $F_B$ into Eqs. (2) and (3), the corrected longitudinal stresses are found.

$$f_c \begin{cases} -0.075 f_1 \\ -0.2825 f_2 \end{cases}$$

$$f_B \begin{cases} +0.376 f_1 \\ +0.416 f_2 \end{cases}$$

$$f_A \begin{cases} -0.688 f_1 \\ -0.208 f_2 \end{cases}$$
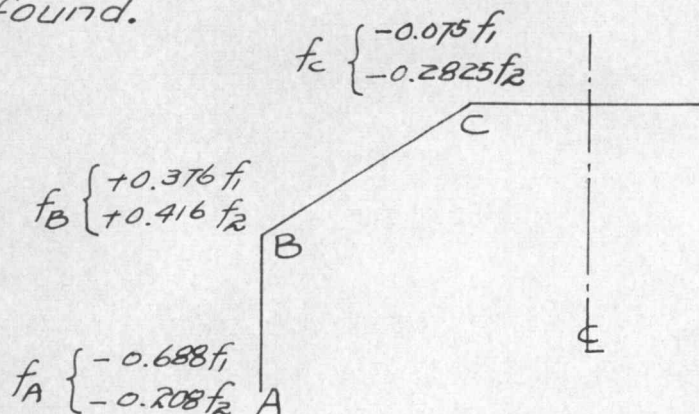
Fig.11 — Corrected Longitudinal Stresses

E. __Case II__
__Considering plate Rotations__
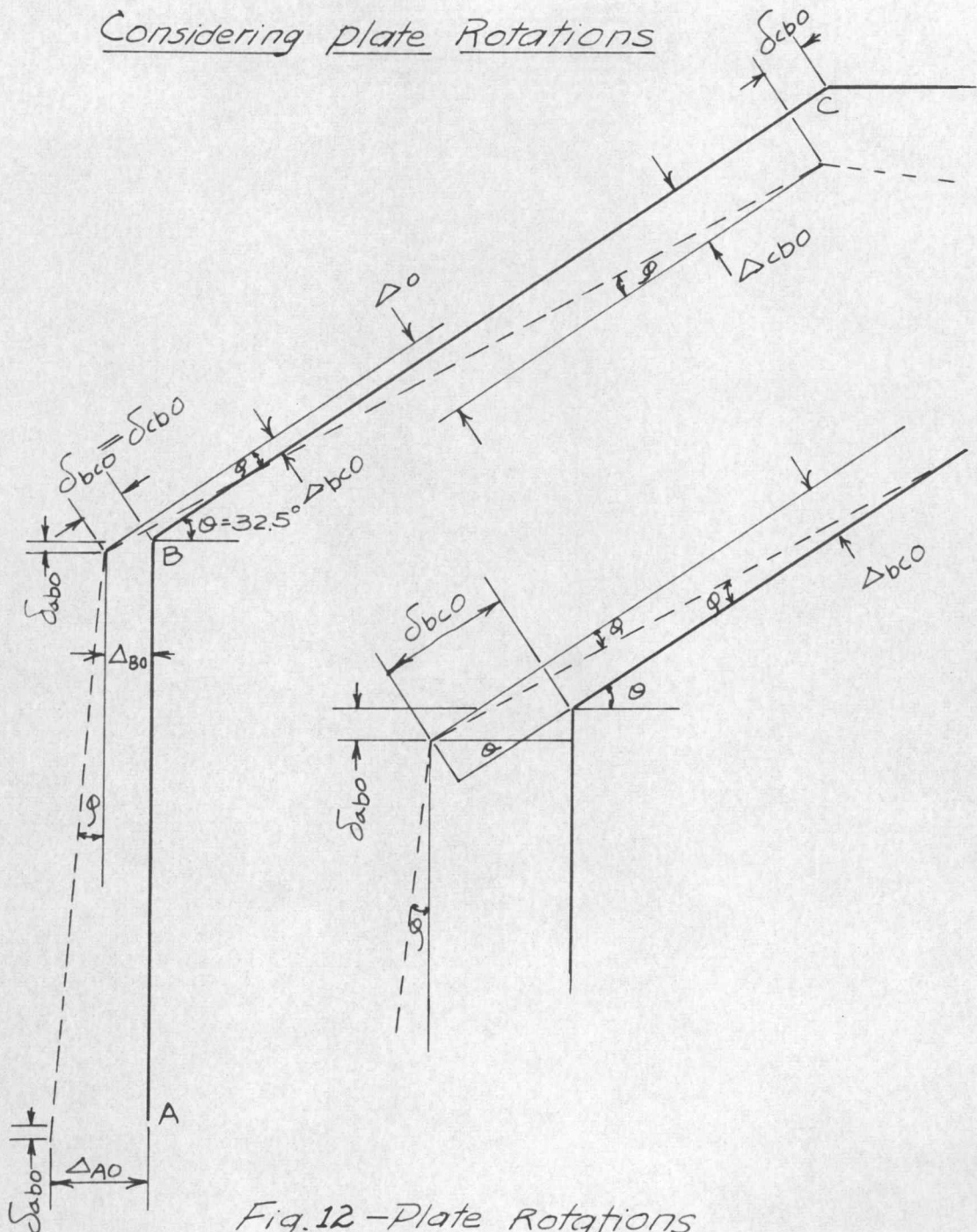


Fig.12 — Plate Rotations

Assuming the outer plate, AB, to rotate freely,

F.E.M. at C, $M_{CF} = \dfrac{3EI_1}{h}(0-\varphi) = -\dfrac{3EI_1\Delta_0}{h^2}$

$$= -3Y \qquad \left(Y = \dfrac{EI_1\Delta_0}{h^2}\right)$$

A        B        C

Adjusted R     ③/④     ①/②

F.E.M.     $-3Y$

    $+1.8Y \quad +1.2Y$

Moment     $-1.2Y \quad +1.2Y$

Shear

$\dfrac{1.2Y}{h}$     $\dfrac{1.2Y}{h}$    0

Fig. 13 — Transverse Moment and Shear

$1.884\dfrac{Y}{h}$    $1.2\dfrac{Y}{h}$

$2.23\dfrac{Y}{h}$

$0.765\dfrac{Y}{h}$

$1.2\dfrac{Y}{h}$    $1.42\dfrac{Y}{h}$

$\theta$

B

A
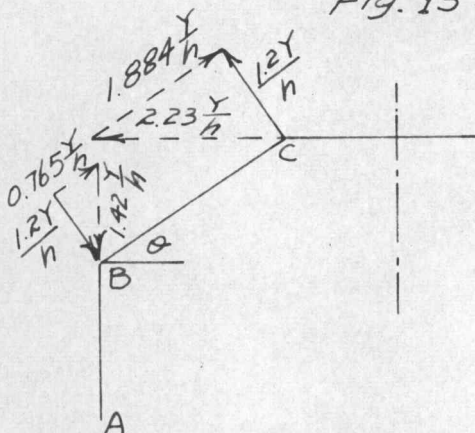
Fig. 14 — Joints Loads and
Its Components

$+2.649\dfrac{Y}{h}$

$\theta$

C

B

$-1.42\dfrac{Y}{h}$

A
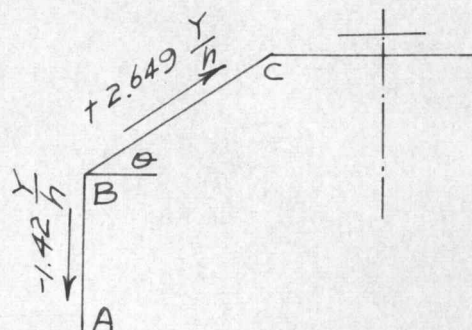
Fig. 15 — $Q'_0$, Plate Loads

If the relative deflection "$\Delta$" is assumed to vary as a sine wave, plate loads also vary as a sine wave.

$$\text{Plate loads. } Q' = Q_0' \sin \frac{\pi x}{\ell}$$

$$M = -\frac{\ell^2 Q_0'}{\pi^2} \sin \frac{\pi x}{\ell}$$

$$\delta = \frac{\ell^4 Q_0'}{\pi^4 EI} \sin \frac{\pi x}{\ell}$$

$$M_0 = -\frac{\ell^2 Q_0'}{\pi^2} \sin \frac{\pi \frac{\ell}{2}}{\ell} = -\frac{\ell^2 Q_0}{\pi^2}$$

| Plate | $M_0$, lb-in | Section Modulus, $Z$, in$^3$ | Stresses, psi |
|-------|--------------|------------------------------|---------------|
| $AB$ | $(\ell/\pi)^2 (1.42\, Y/h)$ | $Z = 0.782$ | $\pm\, f_1' = 110.7\, Y$ |
| $BC$ | $(\ell/\pi)^2 (-2.649\, Y/h)$ | $Z = 1.5$ | $\pm\, f_2' = 107.5\, Y$ |
| $CC'$ | | $Z = 1.5$ | $0$ |

TABLE 2 —Computation of the Longitudinal Stresses



$+f_2'$  $O$
$C$
$-f_2'$
$-f_1'$  $B$
$\mathcal{C}$
$+f_1$  $A$

Fig. 16—Longitudinal Stresses

$f_c' \begin{cases} +0.075\, f_1' \\ +0.2825\, f_2' \end{cases}$

$C$

$f_B' \begin{cases} -0.376\, f_1' \\ -0.416\, f_2' \end{cases}$

$B$

$\mathcal{C}$

$f_A' \begin{cases} +0.688\, f_1' \\ +0.208\, f_2' \end{cases} A$
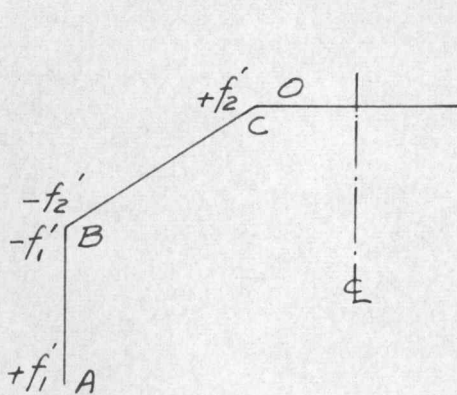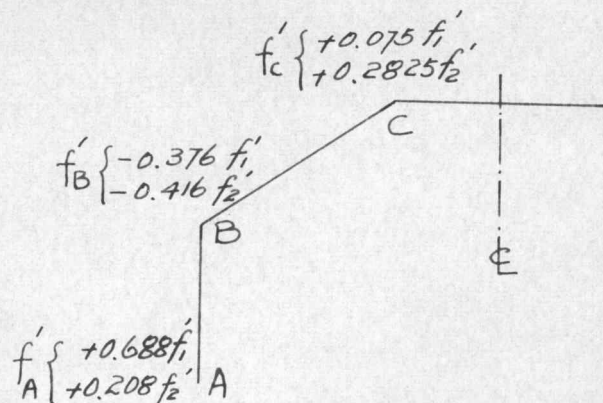
Fig. 17 —Corrected Longitudinal Stresses

## F. Deflection Formulas

For plate $AB$.

$$\delta_1 = \frac{\ell^4 Q_0}{\pi^2 E I} \sin \frac{\pi x}{\ell}$$

$$\delta_{10} = \frac{\ell^2 M_0}{\pi^2 E I} = \left(\frac{\ell^2}{\pi^2 E I}\right)\left(\frac{fI}{C}\right)$$

$$= \left| \frac{\ell^2 (f_A - f_B)}{\pi^2 E h_1} \right| \uparrow$$

$$\delta_{10}' = \left| \frac{\ell^2 (f_A' - f_B')}{\pi^2 E h_1} \right| \downarrow$$

The values of the deflection "$\delta$" are absolute, and arrows designate the direction or sign. These arrows are replaced by positive or negative signs according to the assumed direction of the deflected structure.

$$\delta_{ab0} = -\left|\delta_{10}\right| + \left|\delta_{10}'\right|$$

$$= \frac{\ell^2}{\pi^2 E h_1} \left[ \left|f_A' - f_B'\right| - \left|f_A - f_B\right| \right] \tag{4}$$

Similarly for plate $BC$,

$$\delta_{bc0} = \frac{\ell^2}{\pi^2 E h} \left[ \left|f_B - f_C\right| - \left|f_B' - f_C'\right| \right] \tag{5}$$

$$\Delta_{bco} = \tan\theta\left(\delta_{bco} - \frac{\delta_{abo}}{\sin\theta}\right) \tag{6}$$

$$\Delta_{cbo} = \delta_{cbo}\cot\theta \tag{7}$$

$$\Delta_o = \Delta_{bco} + \Delta_{cbo}$$

$$= \delta_{cbo}(\tan\theta - \cot\theta) - \frac{\delta_{abo}}{\cos\theta}$$

$$= \frac{\ell^2}{\pi^2 E}\left[\left(|f_B - f_C| - |f_B' - f_C'|\right)\left(\frac{\tan\theta + \cot\theta}{h}\right)\right.$$

$$\left. - \left(\frac{1}{\cos\theta\, h_1}\right)\left(|f_A' - f_B'| - |f_A - f_B|\right)\right] \tag{8}$$

## G. Computation of the Final Longitudinal Stresses

For case II,

$$\left.\begin{aligned} f_1' &= \pm\left(\frac{\ell^2}{\pi^2}\right)\left(1.42\,\frac{Y}{h}\right)\left(\frac{1}{Z_{AB}}\right) \\[2ex] f_2' &= \pm\left(\frac{\ell^2}{\pi^2}\right)\left(2.649\,\frac{Y}{h}\right)\left(\frac{1}{Z_{BC}}\right) \end{aligned}\right\} \tag{9}$$

Using Eq. (8),

$$\Delta_o = \frac{\ell^2}{\pi^2 E}\left[\left(\frac{\tan 32.5° + \cot 32.5°}{6}\right)(0.451\,f_1 + 0.6985\,f_2\right.$$

$$\left.- 0.451\,f_1' - 0.6985\,f_2'\right) - \left(\frac{1}{\cos 32.5°}\right)\left(\frac{1}{4.33}\right)$$

$$\left. \left(1.064\,f_1' + 0.624\,f_2' - 1.064\,f_1 - 0.624\,f_2\right)\right]$$

$$= \frac{\ell^2}{\pi^2 E}\left(2,035 - 0.458\,f_1' - 0.428\,f_2'\right) \qquad (10)$$

Substituting $Y = \frac{EI\Delta_o}{h}$ into Eq. (9),

$$\Delta_o = \frac{(\pi^2 f_1' h^3 Z_{AB})}{(\ell^2)(1.42\,EI_\perp)}$$

$$\frac{f_1'}{f_2'} = \frac{1.42\,Z_{BC}}{2.649\,Z_{AB}} = 1.03 \qquad (11)$$

Solving Eqs. (10) and (11),

$$f_1' = 1,820 \text{ psi}, \qquad f_2' = 1,770 \text{ psi}$$

The final longitudinal stresses are found by superposing the corrected longitudinal stresses of two cases.

However, $|f_A - f_B| = 3,118$ psi is larger than $|f_A' - f_B'| = 3,059$ psi. Therefore, $\delta_{abo}$ becomes negative sign which does not agree with the assumed deflected structure in Fig. 12.

*Deflected structure with vertical upward displacement of the plate AB will be tried.*



Fig. 18 — Correct Plate Rotations

$$\delta_{abo} = \frac{\ell^2}{\mathcal{I}^2 Eh_1}\Big[\,|\,f_A - f_B\,| - \lceil\,f_A' - f_B'\,\rceil\,\Big] \qquad (4)'$$

$$\delta_{bco} = \frac{\ell^2}{\mathcal{I}^2 Eh}\Big[\,|\,f_B - f_C\,| - |\,f_B' - f_C'\,|\,\Big] \qquad (5)$$

From the geometric relations in Fig. 18,

$$\Delta_{bco} = \left( \delta_{bco} + \frac{\delta_{abo}}{\cos 57.5°} \right) \cot 57.5° \qquad (6)'$$

$$\Delta_{cbo} = \delta_{bco} \cot \theta \qquad (7)$$

$$\delta_{abo} = \frac{\ell^2}{\pi^2 E h_1} \left[ 3,151 - 0.624 f_2' - 1.064 f_1' \right]$$

$$= \frac{\ell^2}{\pi^2 E h_1} \left[ 3,151 - 185.1 Y \right]$$

$$\delta_{bco} = \frac{\ell^2}{\pi^2 E h} \left[ 3,184 - 125.0 Y \right]$$

$$\Delta_o = \delta_{bco} + \Delta_{cbo}$$

$$= \frac{\ell^2}{\pi^2 E} \left[ \frac{1.186}{h_1} (3,151 - 185.1 Y) \right.$$

$$\left. + \frac{2.2071}{h} (3,184 - 125.0 Y) \right]$$

Since $Y$ equal to $\frac{E I_1 \Delta_o}{h^2} = 148 \Delta_o$,

$$\Delta_o = \frac{\ell^2}{\pi^2 E} \left[ 2,035 - 14,330 \Delta_o \right]$$

$$= 0.1087 \quad in.$$

$$Y = 16.1 \quad in.$$

The final longitudinal stresses are given Table 3.

| Edge | Case I, f psi | Case II, f' psi | Final Stresses (Case I + Case II) psi |
|------|------|------|------|
| C | −1,237 | +621 | −618 |
| B | +1,945 | −1,388 | +557 |
| A | −1,206 | +1,581 | +375 |

TABLE 3 — Final Longitudinal Stresses

## H. Deflection Computations

$$\delta_{abo} = \frac{\ell^2}{\pi^2 E h_1}\left[\, |f_A - f_B| - |f_A' - f_B'| \,\right]$$

$$= \frac{(60)^2}{(\pi^2)(1.6\times10^6)(4.33)}\,[\,182\,] = 0.0096 \text{ in.} \uparrow$$

$$\delta_{bco} = \frac{\ell^2}{\pi^2 E h_1}\left[\, |f_B - f_C| - |f_B' - f_C'| \,\right] = 0.0447 \text{ in.} \downarrow$$

$$\triangle_{co} = \frac{\delta_{cbo}}{\sin 32.5°} = 0.0832 \text{ in.}$$

$$\triangle_{Bo} = \frac{\delta_{abo}}{(\sin 32.5°)(\cos 32.5°)} = 0.0212 \text{ in.}$$

$$\triangle_{Ao} = \triangle_{Bo} + h_1 \varphi = 0.0212 + (h_1)\left(\frac{\triangle_o}{h}\right) = 0.0999 \text{ in.}$$
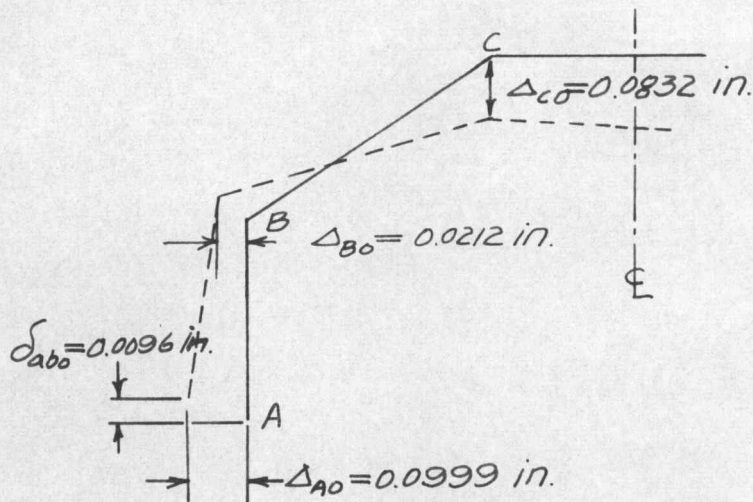
Fig. 19 — Displacements at Middle Section

I. <u>Longitudinal</u> <u>Stresses</u> <u>(out of plane)</u> <u>at</u>
<u>the</u> <u>Edges</u> <u>of</u> <u>Plate</u>

Assuming that the deflections perpendicular to
the plates vary as a half sine wave
longitudinally, unequal longitudinal (out of plane)
stresses at each joint will be found.

At joint C,

$$\Delta_{cb} = \Delta_{cbo} \, Sin \frac{\pi x}{\ell} = \left( \delta_{bco} \, Cot \, 32.5° \right) Sin \frac{\pi x}{\ell}$$

$$M_o = EI \, \Delta_{cbo} \frac{\pi^2}{\ell}$$

$$f_{cB} = \frac{M_o C}{I} = \frac{(1.6 \times 10^6)(10.07)(\pi^2)}{(4 \times 60)^2} = 76.5 \, psi$$

$$f_{cc'} = \frac{(f_{cB})(\Delta_{co})}{(\Delta_{cbo})} = \frac{(76.5)(0.0832)}{(0.07)} = 91.0 \text{ psi}$$

At joint B,

$$f_{BC} = (f_{cB})\left(\frac{\Delta_{bco}}{\Delta_{cbo}}\right) = (f_{cB})\frac{(\Delta_o - \Delta_{cbo})}{(\Delta_{cbo})} = 42.3 \text{ psi}$$

$$f_{BA} = (f_{cB})\frac{(\Delta_{Bo})}{(\Delta_{cbo})} = (76.5)\frac{(0.0212)}{(0.07)} = 23.2 \text{ psi}$$

At edge A,

$$f_{AB} = (f_{cB})\frac{(\Delta_{Ao})}{(\Delta_{cbo})} = (76.5)\frac{(0.0999)}{(0.07)} = 108.0 \text{ psi}$$
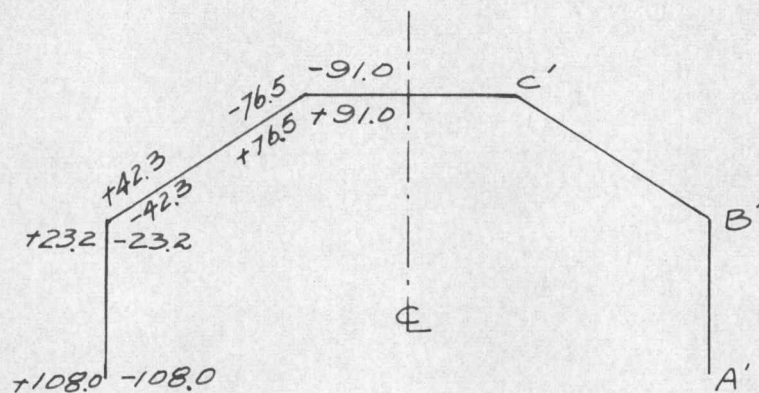


Fig. 20 — Longitudinal (out of plane) Stresses, psi

J.   Transverse Moments

The bending moments in a transverse 1.0 inch wide strip are found by superposing the moments in two cases. In case I, in which

external loads and unyielding supports considered,
the connecting moment at joint C is
$M_{CO}=0.05 P_0 h^2 = 5.04$ lb-in. The maximum
moment with uniform load in span CC' is
$\frac{P_0 h^2}{8} = 12.6$ lb-in. In case II, the moment
due to the plate rotations is $M'_{CO}=1.2Y= 19.3$ lb-in.

| Joint | Case I Lb-In. | Case II Lb-In. | Final Moments (Case I + Case II) Lb-In. |
|---|---|---|---|
| C | 5.04 | -19.3 | -14.26 |
| B | 0 | 0 | 0 |

TABLE 4 —Transverse Moments in 1.0 inch Strip
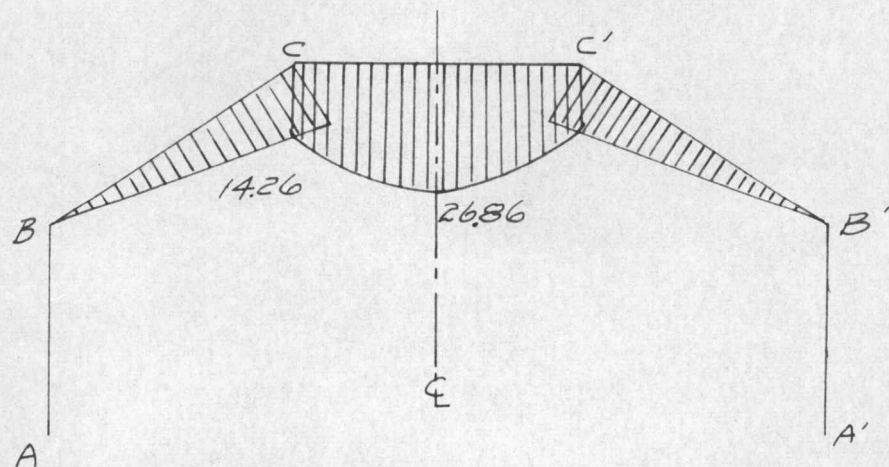


Fig. 21 —Transverse Moments, Lb-In.

PART IV

EXPERIMENTAL INVESTIGATION
OF A PLYWOOD MODEL

A.  Model Description

The material descriptions and strength properties are
mentioned in p. 9.  For loading six copper plates weighing
5.5 pounds each were placed, as one layer, over the top
horizontal plate.  These layers were stacked until the
desired weight was loaded as shown in Fig. 2 2.

The edges of plates at the joints are not rectan-
gular shape and dimensions are measured along the center-
line of the plate cross section as shown in Fig. 24.
The plates were glued at the joints and nailed at six
inch intervals.  The bottoms of the end diaphragms were
also glued and nailed in order to prevent "tip-in" action
which would cause the end diaphragms to bend inward as
the load is applied.  Ames dial gages were installed at
edges A and C to determine vertical deflections; at edges
A, B, and quarter point of the bottom of the edge beam
for horizontal deflections; and at the top of end dia-
phragm for horizontal "tip-in" action.  SR-4 strain gages
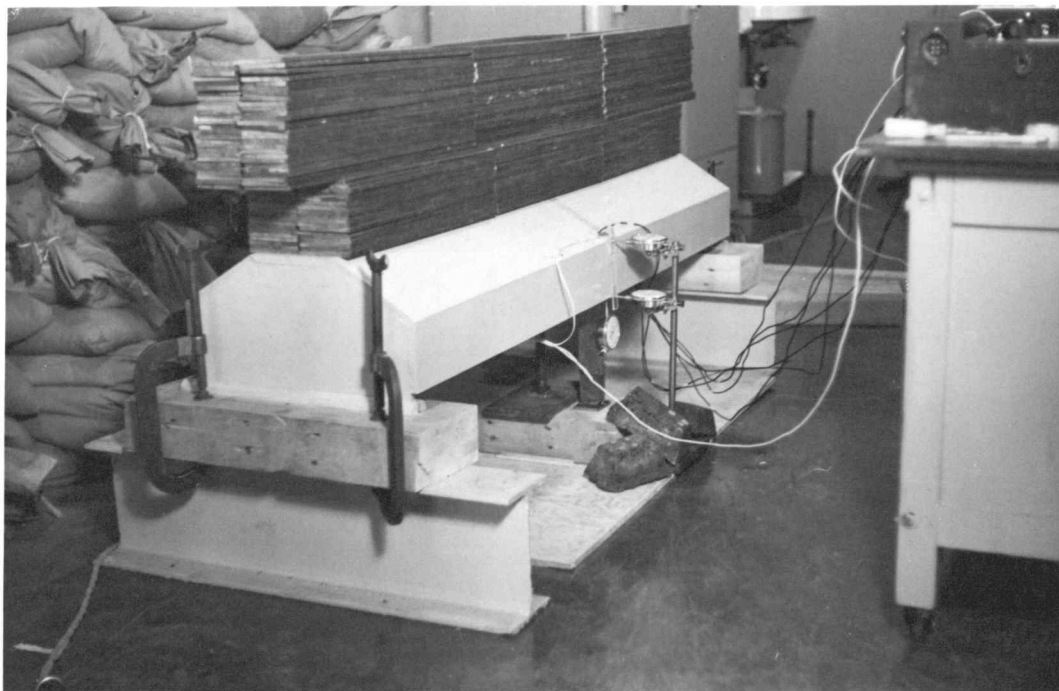
Figure 22

Loaded Model with Gages

were placed at the joints, free edge, and center of the
plate CC' for longitudinal strains; a transverse SR-4
strain gage was placed at the bottom of the joint C as
shown in Fig. 24. In Fig. 23, 1, 2, 3, 4, 5, 6, and 7
are the longitudinal strain gages and 8 the transverse
gage. The picture in Fig. 22 does not show the Ames dial
gages at the top of the end diaphragm and quarter point of
the edge beam, nor does it show strain gages 2 and 6.
These strain gages were wired independently to give the
strain readings at outer and inner surfaces of the plate
separately.

B.  Experimental Procedure

The first experiment was made by increasing loads
100 pounds at a time up to a total of 800 pounds. Gage
readings were recorded at 100 pound increments. In the
second experiment, loads were applied at 200 pound incre-
ments up to 800 pounds, then at 50 pound increments up to
a total of 1,950 pounds. At each loading interval the
gage readings were taken. The third experiment with the
loading increments of 200 pounds were run increasing the
load to 800 pounds. From 800 pounds up to a total of

A

P

A

B

$\omega_j$

SR-4 Strain Gages

B

$\ell = 60$ In.

Section A-A

6.0 In.

6.0 In.

4.33 In.

Dimensions of Cross Section

6

5  8     T

4

3

2   1

Section B-B

Fig. 23 — Plywood Model

C

6.0 In.

6.0 In.

5/64"
8/64"
6/64"
8/64"
5/64"

B

32.5°

4.33 In.

*Veneer Thickness of*
*½ In. Plywood Sanded*

3/8"

3/8"

C

3/4"

B

⅓"

1"

A

*Joint Connections*

*Locations of SR-4 Strain Gages*
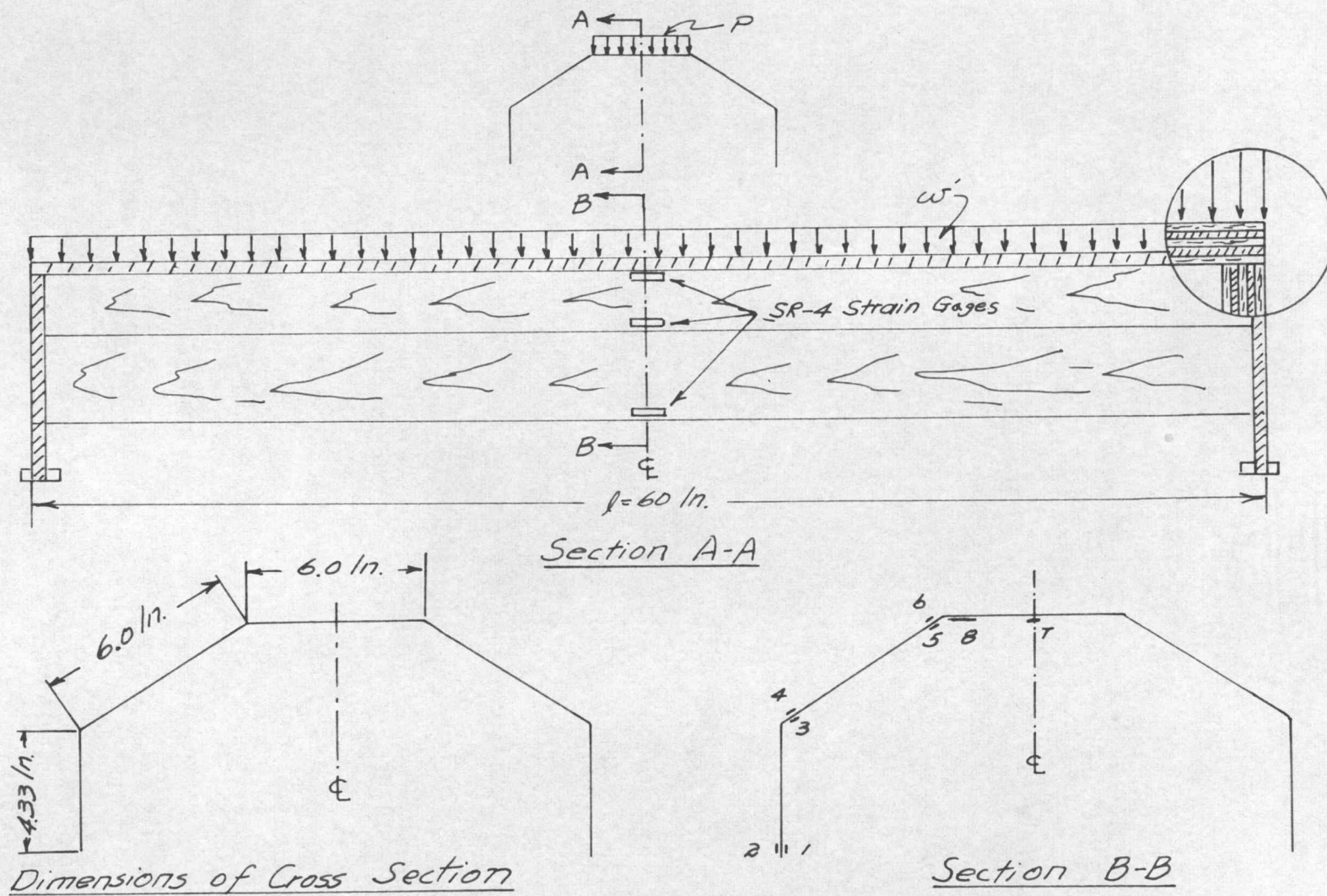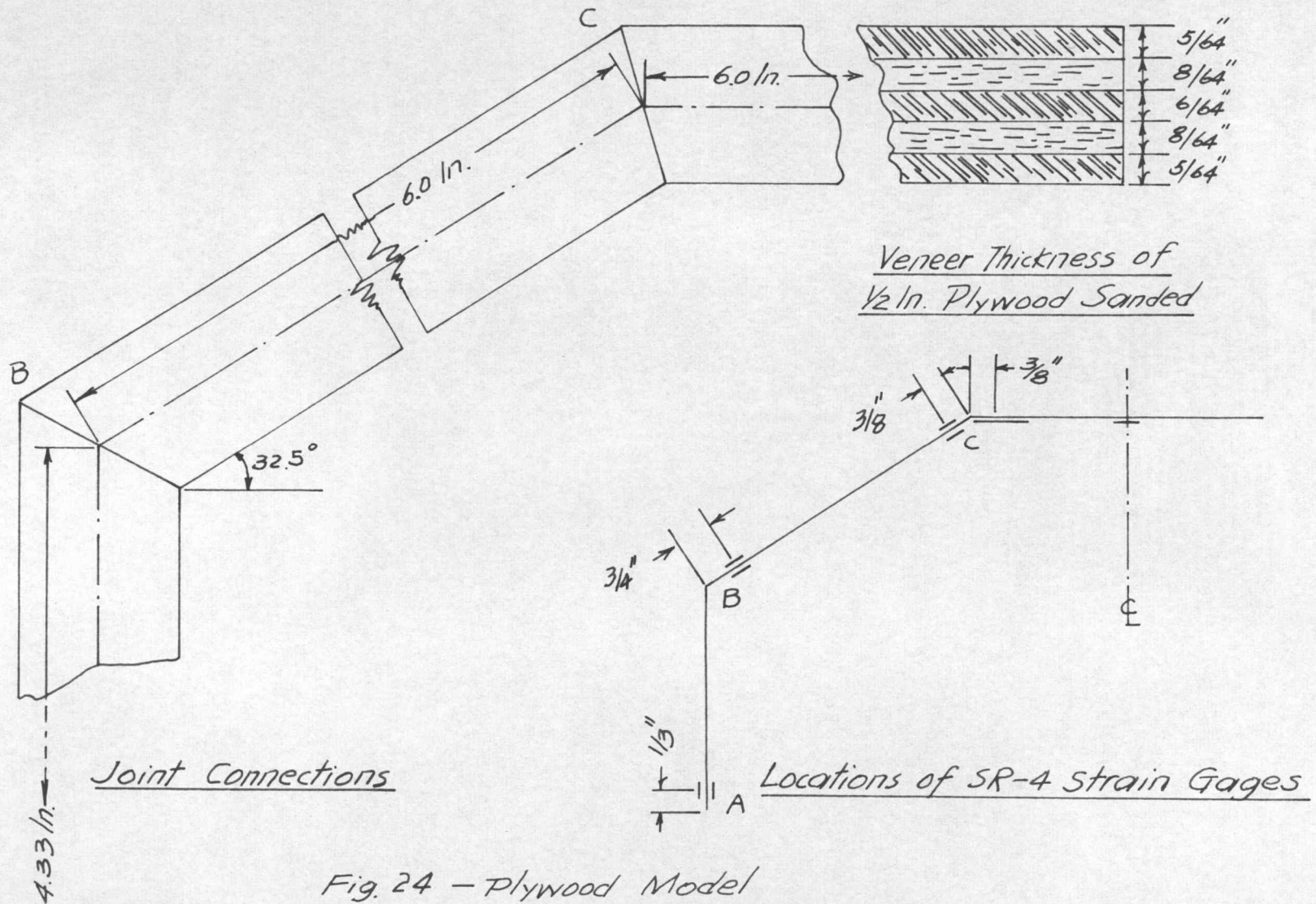
*Fig. 24 — Plywood Model*

1,600 pounds, the load was added at one time and the gage readings were taken only once.

C. Results

### 1. Observations of gage reading

Immediately after each loading, it was observed that both strain and Ames dial gage readings were creeping rapidly for about one and one-half minutes, then steadying. It is believed that this creep is caused by the fact that certain time is required for plastic flow and joint translations to occur. The gage readings in the experiment were taken after an elapsed time of approximately two minutes.

### 2. Strain Measurements

The longitudinal and transverse strains at the middle section of the model are shown in Fig. 26. For the plate CC', a top surface strain gage was not installed because of the difficulty caused by the loading on the top of the plate. Longitudinal plate stresses were found from the average strain values of the inner and outer surface of the plate. A transverse strain of 350 micro-in./in. was measured

37
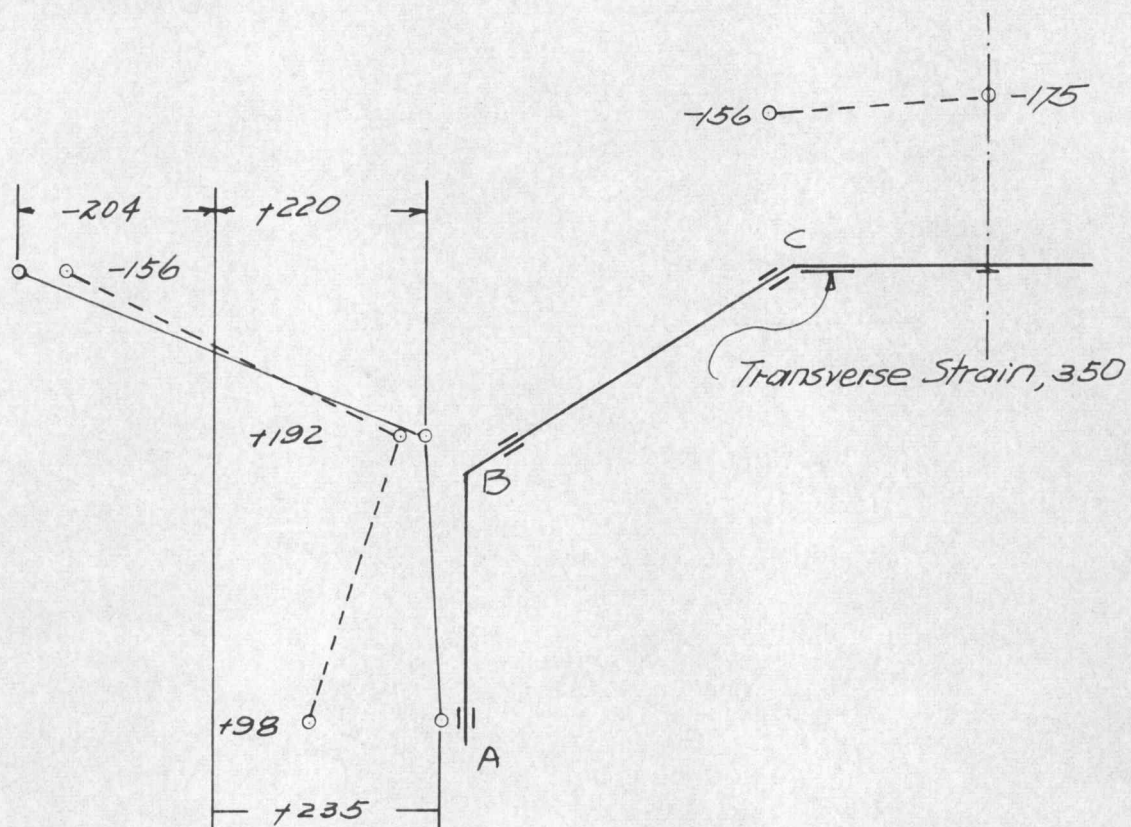


Fig. 25 — Maximum Longitudinal Strain, $\frac{Micro\text{-}Inch}{Inch}$
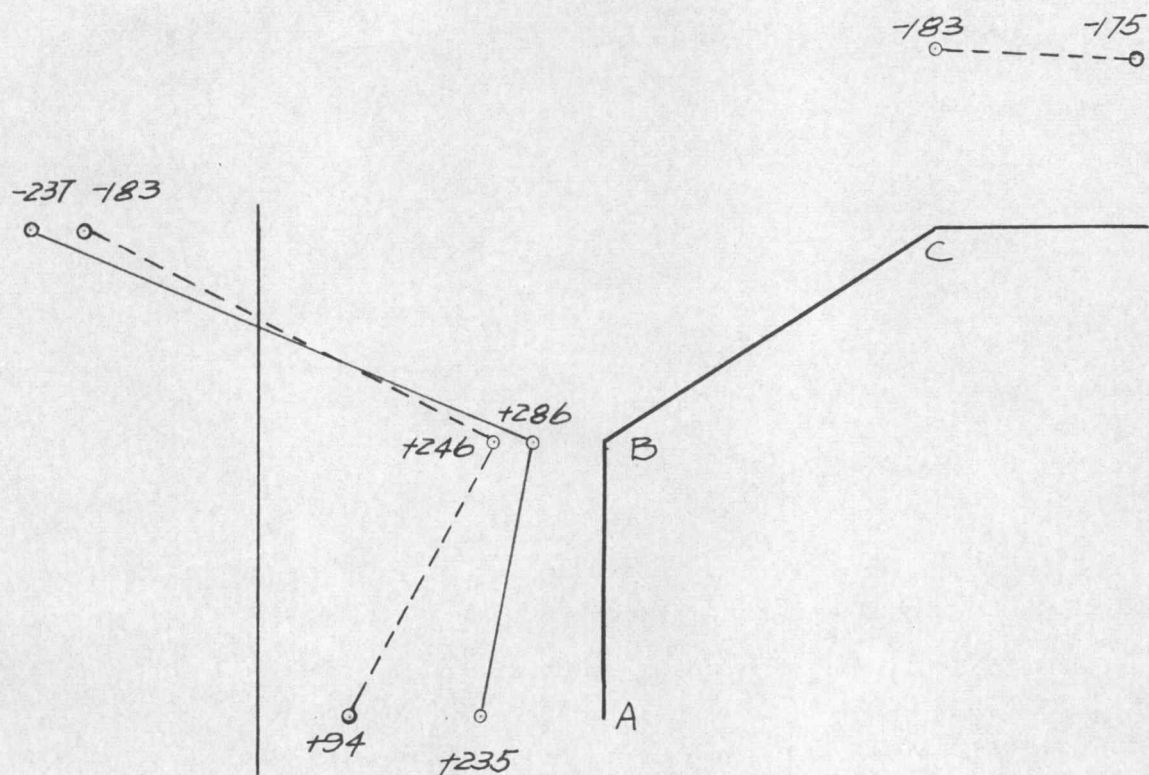
Fig. 26 — Maximum Longitudinal Strain
at the Joint , $\dfrac{\text{Micro-Inch}}{\text{Inch}}$

Note :

    Dotted lines are for inner surface
    Solid lines are for outer surface

at joint C.  Transverse moment in center strip of the

model yields as the connecting moments at the joint

C,  $M_{co} = \epsilon E L / C = (350)(1.6)(0.0033)/0.25 = 7.42 \, lb\text{-}in.$

As the transverse deflection in span CC' is negli-

gible due to the short span length compared to the

longitudinal length of the model, this 7.42 lb.-in.

is considered as an average moment.
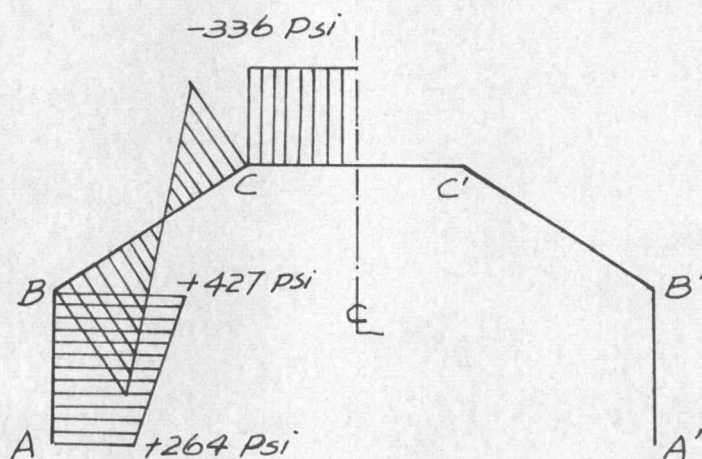
Fig. 27—Final Longitudinal Edge Stresses

## 3.  Displacement Measurements

The measured displacements of the edges are shown

in Fig. 28.  The values of $\triangle_A$ and $\triangle_{AO}$ verify the

previous assumption that the deflections perpendic-

ular to the plate vary as a half sine wave.  The

downward vertical displacement of the plate AB does

$\Delta_A = 0.100''$

$\frac{\ell}{4}$

$\frac{\ell}{4}$

C

B

$\Delta_{CO} = 0.096''$

$\Delta_{BO} = 0.058''$

A

$\delta_{abo} = 0.0095''$

$\Delta_{AO} = 0.1365''$
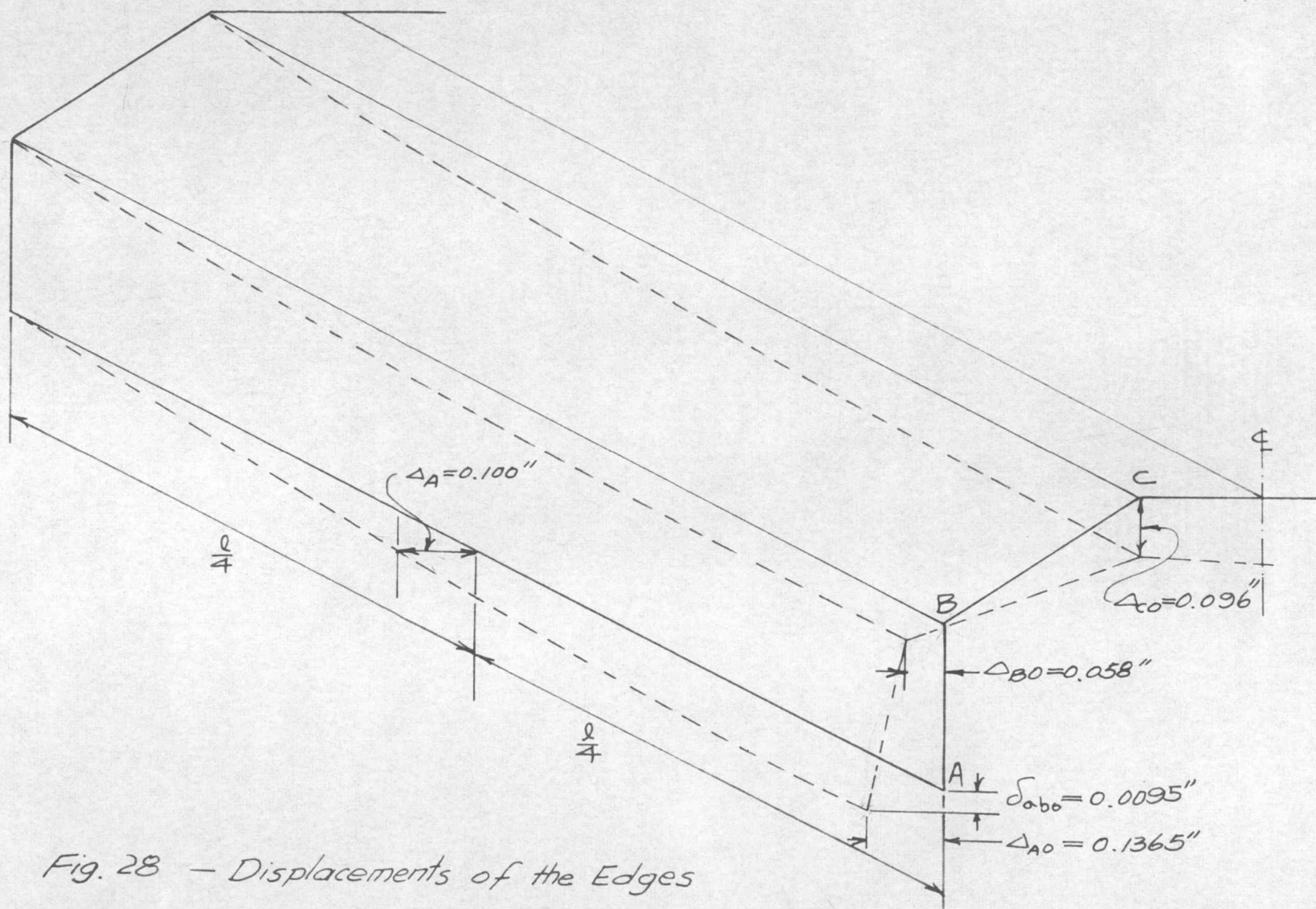
Fig. 28 — Displacements of the Edges

40

not agree with the theoretical displacement which
is upward.

The possible causes of this disagreement which
at present can be offered are, that the wooden block
under the end diaphragm compressed as the load was
applied and the glued joints were not rigid enough
to translate the connecting moments fully.  Since
the longitudinal (out of plane) stresses are of the
same order of magnitude as the deflections, it is not
necessary to compute the longitudinal (out of plane)
stresses for the comparison of theoretical and
experimental values.

PART V

## DISCUSSIONS ON THE RESULTS OF THE
## EXPERIMENTAL AND THEORETICAL INVESTIGATION

In ordinary beam theory the longitudinal stresses
are proportional to the distances from the centroid of
the entire section, whereas they are not proportional in
hipped plate theory.

| (1) Edge | Stresses, Psi | | |
|---|---|---|---|
| | (2) Ordinary Beam Theory | (3) Hipped Plate Theory | (4) Experimental Values |
| C | -340 | -618 | -336 |
| B | +180 | +557 | +427 |
| A | +867 | +375 | +264 |

Table 5 - Maximum Longitudinal Stresses

| Edge | Plate | Types of Deflections | Deflection by Hipped Plate Theory, Inch | Deflection by Test, Inch |
|---|---|---|---|---|
| A | AB | $\delta_{abo}$ | 0.0096 | -0.0095 |
| A | AB | $\triangle_{AO}$ | 0.0999 | 0.1365 |
| B | BA | $\triangle_{BO}$ | 0.0212 | 0.058 |
| C | CC' | $\triangle_{CO}$ | 0.0832 | 0.096 |

Table 6 - Deflections at the Middle Section

In other words, the hipped plate structures do not behave as a unit. Thus beam theory cannot be applied directly to the structures of nonhomogeneous material, not to the hipped plate structures. However, the beam theory gives the right sense of the signs of the stresses as shown in Table 5. The longitudinal stress values by hipped plate theory are much higher than the experimental values. Assuming that theoretical stresses in column (3) of Table 5 are the correct values, the errors of the longitudinal stresses at the edges A, B and C are:

$$\frac{375 - 264}{375} \times 100 = +30\%, \quad \frac{557 - 427}{557} \times 100 = 23\%$$

and $\frac{618 - 336}{618} \times 100 = 46\%$.

The possible causes for these errors are as follows:

A.  During the experiment, a slight twist of the model was observed.

B.  The material is nonhomogeneous, nonmonolithic, and nonisotropic.

C.  In theoretical analysis, strength property calculations of the plywood might not be exactly

correct, even though the model was designed in accordance with the specification by the Douglas Fir Plywood Association.

D. The joints are probably not completely homologous.

E. The glued connected joints were not stiff enough to be regarded as rigid joints.

F. The cross sections of the plate at joints were not rectangular.

G. The effect of nonuniform loading due to overhang of top bars and possible bridging.

The computed maximum transverse moment at joint C is 7.42 pound-inches by test and 14.26 pound-inches computed by the hipped plate theory. The displacements of the edges are listed in Table 6 for comparison. Since the transverse moments, longitudinal stresses, and deflections of the edges are of the same order of magnitude, the errors in transverse moments and deflections of the edges probably result from the above causes.

The deflections perpendicular to the plate are important in the hipped plate analysis. This type of deflection is the main cause of the different strains in the inner and outer surfaces of the plate. Since the

difference in longitudinal strains between the inner
and outer surfaces is twice the longitudinal (out of
plane) strains, from Fig. 26 the approximate longitudinal
(out of plane) stresses can be computed. At the edges
A, B, and C the longitudinal (out of plane) stresses are:

$$\left(\frac{235 - 94}{2}\right)(1.6) = 113, \quad \left(\frac{286 - 246}{2}\right)(1.6) = 32, \text{ and}$$

$$\left(\frac{237 - 183}{2}\right)(1.6) = 43 \text{ psi.}$$ These values agree quite
well with the computed values of the theoretical analysis
in Fig. 20 except at the edge C. By computation,
assuming deflections as a sine wave, at the edge C the
longitudinal (out of plane) stress is:

$$f_{cc'} = \frac{EI \Delta_{co} z^2 c}{I \ell^2} = 104.0 \text{ psi}$$

The equation of the longitudinal (out of plane)
stresses is expressed as:

$$f_{cc'} = \frac{EI \Delta z^2 c}{I \ell^2} = k \Delta = k'(P_0, Q_0) = k''(P_0 - Q_0) \quad (12)$$

The curves of the load versus strain at the joints are
linear except at the edge A. This statement of the
linear relationship between load and strain, agrees with
the equation (12) by theory.

Fig. 29
Strains at The Middle
Section of The Model

Fig. 30
Deflections at The Middle
Section of The Model
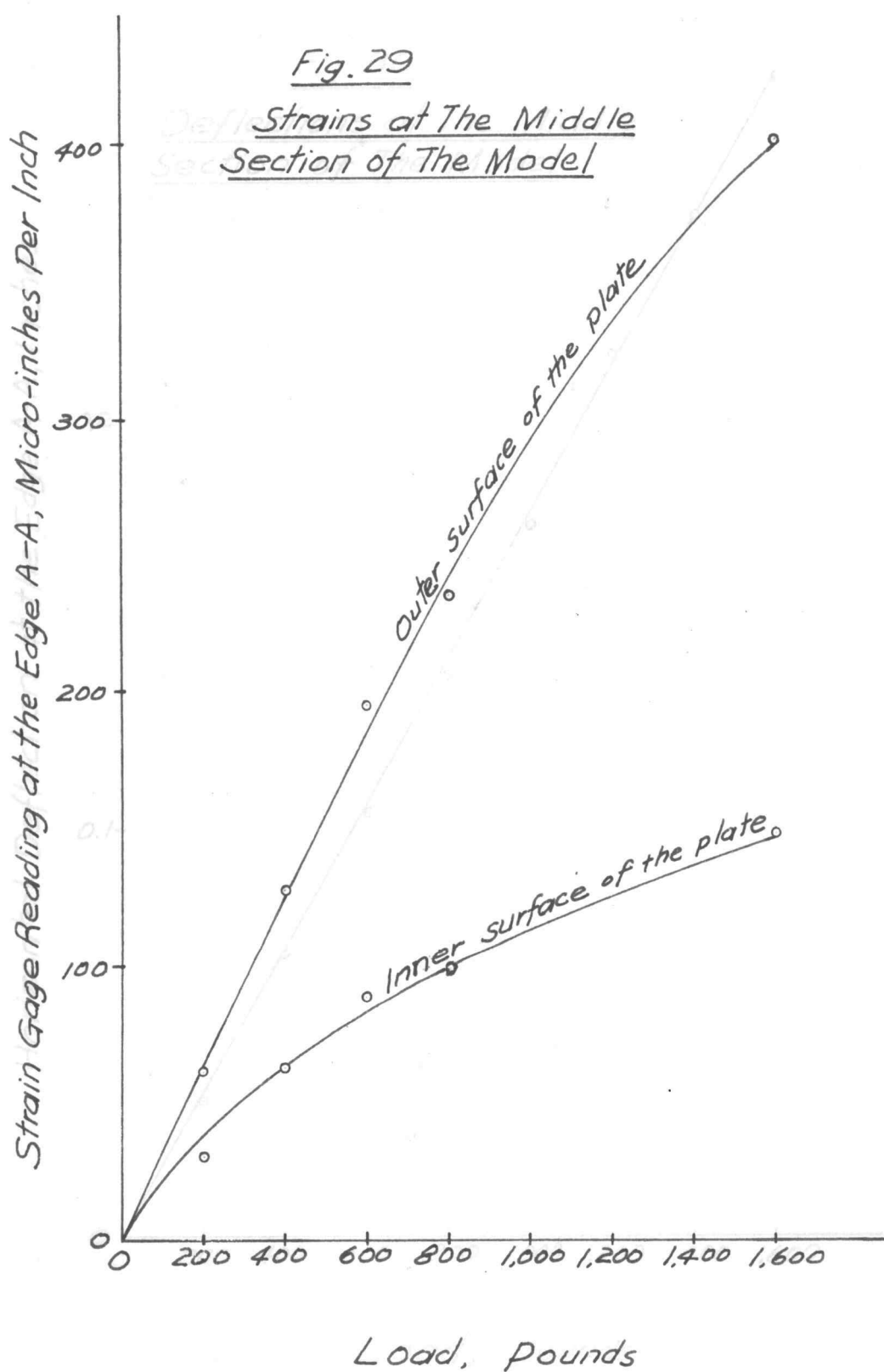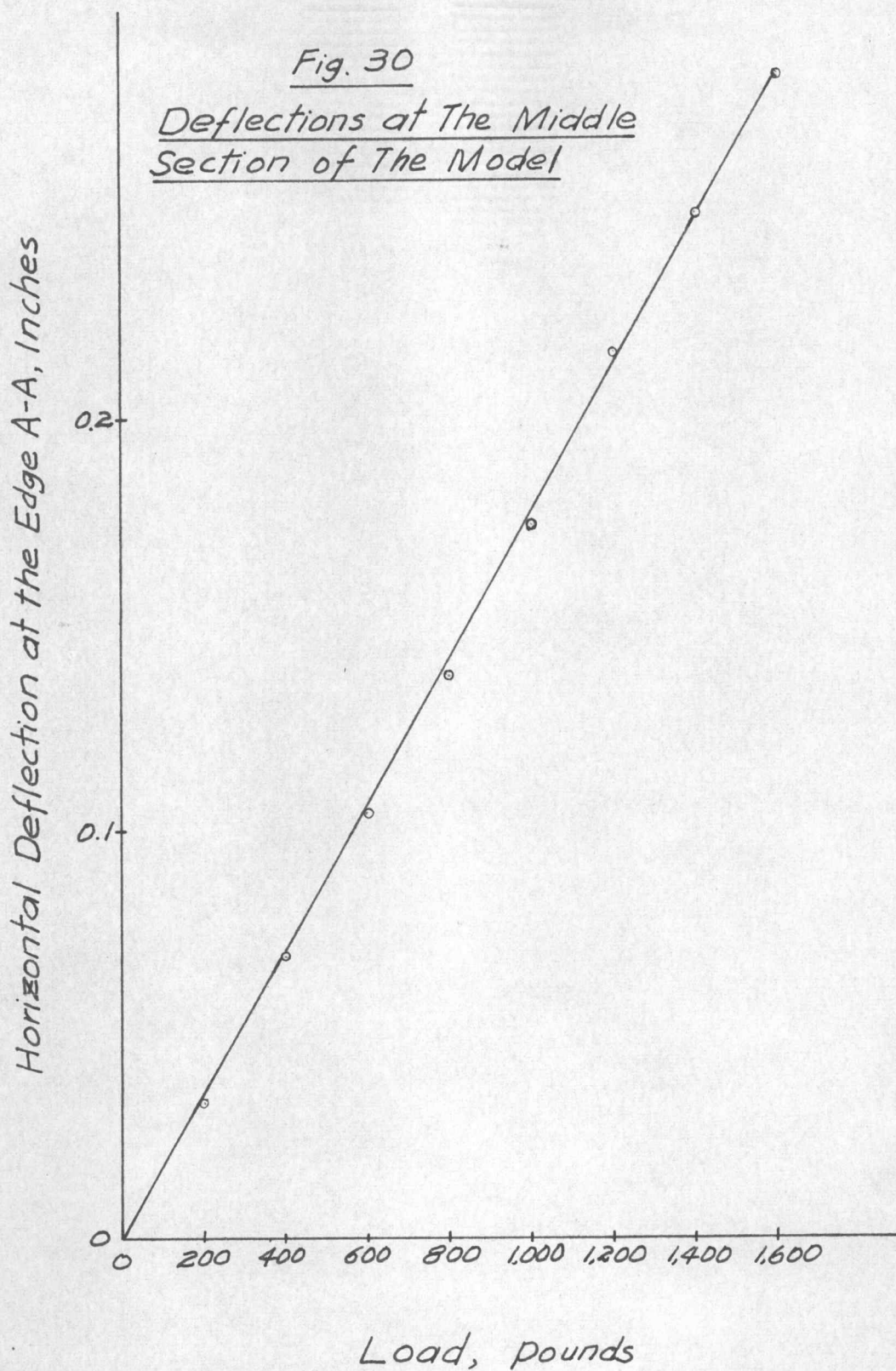
At the edge A, however, the load versus strain curve
is not linear despite the linear relationship between load
and deflection as shown in Fig. 29 and Fig. 30.  In Fig.
29, up to about 1,000 pounds the load versus strain curve
is linear.  Beyond 1,000 pounds, in the writer's opinion,
some unknown factors are complicating the method of
analysis presented in this paper.  Possibly this non-
linearity beyond 1,000 pounds might be due to the same
causes of the errors in the longitudinal stresses.

# PART VI

## CONCLUSIONS

If the properties of plywood were more uniform and
more reliable data on plywood were available, a plywood
model would be easy to build and satisfactory for studying
the hipped plate structures. Rigid joint connections are
also essential for perfect model construction.

Since $\triangle_{AO} = \triangle_o \sin \frac{\pi x}{\ell} = \phi(\delta, \triangle)$ is fairly
well verified by the experiment, the assumption made in
the theoretical analysis, in which the elastic line of the
plate along the longitudinal edges is expressible as
functions of $\sin \frac{\pi x}{\ell}$ , is confirmed. As the load is
increased the effects of the longitudinal (out of plane)
stresses appear to be dominant.

It is believed that the proposed theory presented
in this thesis describes more completely the structural
action of hipped plate structures than most methods
currently used in design. It is hoped that further
testing may aid in verifying this theory and expanding
upon obscure points.

BIBLIOGRAPHY

1.  American Society of Civil Engineers. Design of cylindrical concrete shell roofs. New York, 1952. 177 p. (ASCE Manuals of Engineering Practice no. 31)

2.  Borg, Sidney F. and Joseph J. Gennaro. Advanced structural analysis. Princeton, New Jersey, D. Van Nostrand, 1959. 368 p.

3.  Douglas Fir Plywood Association. Technical data on plywood. Tacoma, 1948. 92 p.

4.  Gaafar, I. Hipped plate analysis considering joint displacements. Transactions of the American Society of Civil Engineers 119:743-784. 1954. (Paper no. 2697)

5.  Miller, Fredric H. Partial differential equations. New York, John Wiley and Sons, 1941. 259 p.

6.  Seely, Fred B. and James O. Smith. Advanced mechanics of materials. 2d ed. New York, John Wiley and Sons, 1952. 680 p.

7.  Simpson, Howard. Design of folded plate roofs. Proceedings of the American Society of Civil Engineers, Journal of the Structural Division 84:1-21. January, 1958. (Proceeding paper no. 1508)

8.  Timoshenko, S. and J. M. Lessells. Applied elasticity. East Pittsburgh, Westinghouse Technical Night School Press, 1925. 544 p.

9.  Timoshenko, S. Theory of plates and shells. New York, McGraw-Hill, 1940. 492 p.

10.  Whitney, Charles S., Boyd G. Anderson and Harold
     Birnbaum.  Reinforced concrete folded plate construc-
     tion.  Proceedings of the American Society of Civil
     Engineers, Journal of the Structural Division
     85:15-43.  October, 1959.  (Proceeding paper no.
     2219)

11.  Winter, G. and M. Pei.  Hipped plate construction.
     Journal of American Concrete Institute,  January,
     1947 (ACI Proceedings Vol. 43), 505 p.

12.  Yitzhaki, David.  The design of prismatic and
     cylindrical shell roofs.  Amsterdam, North-Holland,
     1959.  253 p.

# A P P E N D I X   A

## TEST DATA

**First Experiment**

| Load Lbs. | Gage Readings, Micro-inches per Inch Gage Number | | | | | |
|---|---|---|---|---|---|---|
| | 1 | 3 | 4 | 5 | 7 | 8 |
| 0 | 5-1340 | 5- 830 | 5- 950 | 5-1140 | 5- 530 | 5- 740 |
| 100 | 1348 | 840 | 5- 978 | 1125 | 518 | 805 |
| 200 | 1360 | 870 | 5-1010 | 1113 | 500 | 860 |
| 300 | 1385 | 910 | 5-1030 | 1100 | 473 | 905 |
| 400 | 1385 | 940 | 5-1080 | 1075 | 460 | 950 |
| 500 | 1405 | 970 | 5-1092 | 1055 | 430 | 990 |
| 600 | 1405 | 997 | 5-1150 | 1030 | 420 | 1030 |
| 700 | 1420 | 1030 | 5-1160 | 1010 | 400 | 1060 |
| 800 | 1423 | 1043 | 5-1200 | 990 | 387 | 1090 |
| Net Strain | +83 | +213 | +250 | -150 | -143 | +350 |
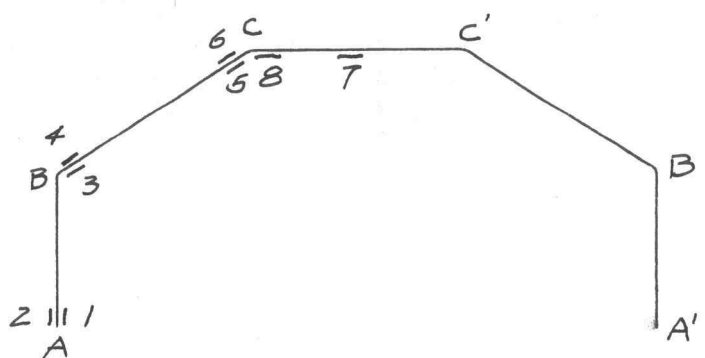


Gages except No. 8 are longitudinal strain
Gage No. 8 is transverse strain

## Deflections at Middle Section
## of the Model

| Load Lbs. | Vertical Deflection Inches Joint | | Horizontal Deflection Inches Joint | |
|---|---|---|---|---|
| | A | C | A | B |
| 0 | | | | |
| | 0.0005 | 0.017 | 0.0155 | 0.0025 |
| 100 | | | | |
| | 0.002 | 0.0135 | 0.0185 | 0.0085 |
| 200 | | | | |
| | 0.0025 | 0.014 | 0.0195 | 0.009 |
| 300 | | | | |
| | 0.0015 | 0.015 | 0.0215 | 0.015 |
| 400 | | | | |
| | 0.0010 | 0.016 | 0.0195 | 0.000 |
| 500 | | | | |
| | 0.0010 | 0.016 | 0.013 | 0.005 |
| 600 | | | | |
| | 0.0020 | 0.013 | 0.021 | 0.008 |
| 700 | | | | |
| | 0.0010 | 0.012 | 0.017 | 0.0075 |
| 800 | | | | |
| Total | 0.0115 | 0.1165 | 0.1455 | 0.0555 |

Second Experiment

| Load Lbs. | Gage Readings, Micro-inches per Inch Gage Number | | | | | |
|---|---|---|---|---|---|---|
| | 1 | 3 | 4 | 5 | 7 | 8 |
| 0 | 1388 | 878 | 1000 | 1190 | 590 | 780 |
| 200 | 1412 | 930 | 1065 | 1158 | 546 | 875 |
| 400 | 1440 | 975 | 1120 | 1118 | 498 | 957 |
| 600 | 1456 | 1010 | 1160 | 1058 | 441 | 1022 |
| 800 | 1486 | 1060 | 1210 | 1035 | 420 | 1100 |
| 900 | 1500 | 1090 | 1235 | 1015 | 400 | 1140 |
| 1000 | 1505 | 1100 | 1260 | 1000 | 390 | 1160 |
| 1100 | 1500 | 1140 | 1295 | 970 | 375 | 1180 |
| 1200 | 1515 | 1158 | 1318 | 950 | 357 | 1210 |
| 1300 | 1523 | 1188 | 1323 | 922 | 335 | 1233 |
| 1400 | 1510 | 1208 | 1372 | 900 | 323 | 1243 |
| 1500 | 1520 | 1232 | 1380 | 870 | 305 | 1255 |
| 1600 | 1520 | 1242 | 1422 | 848 | 295 | 1275 |
| 1700 | 1522 | 1275 | 1430 | 820 | 278 | 1288 |
| 1733 | 1495 | 1285 | 1470 | 803 | 280 | 1273 |
| 1788 | 1498 | 1317 | 1478 | 782 | 270 | 1288 |
| 1843 | 1495 | 1320 | 1515 | 762 | 262 | 1295 |
| 1953 | 1500 | 1360 | 1527 | 730 | 237 | 1323 |
| Net Strain | +112 | +482 | +527 | -460 | -353 | +543 |

| Load Lbs. | Vertical Deflection Inch | | Horizontal Deflection Inch | |
|---|---|---|---|---|
| | A | C | A | B |
| 0 | | | | |
| | 0.003 | 0.0235 | 0.0325 | 0.012 |
| 200 | | | | |
| | 0.002 | 0.025 | 0.0360 | 0.016 |
| 400 | | | | |
| | 0.0025 | 0.0255 | 0.0350 | 0.016 |
| 600 | | | | |
| | 0.0020 | 0.022 | 0.033 | 0.014 |
| 800 | | | | |
| | 0.0005 | 0.0125 | 0.020 | 0.009 |
| 900 | | | | |
| | 0.000 | 0.0115 | 0.017 | 0.007 |
| 1,000 | | | | |
| | 0.001 | 0.015 | 0.019 | 0.008 |
| 1,100 | | | | |
| | 0.000 | 0.013 | 0.023 | 0.011 |
| 1,200 | | | | |
| | 0.001 | 0.011 | 0.017 | 0.007 |
| 1,300 | | | | |
| | 0.000 | 0.015 | 0.023 | 0.010 |
| 1,400 | | | | |
| | 0.0005 | 0.013 | 0.019 | 0.009 |
| 1,500 | | | | |
| | 0.0003 | | 0.0145 | |
| 1,600 | | | | |

Third Experiment

| Load Lbs. | Gage Readings, Micro-inches per Inch Gage Numbers | | | | | | | |
|---|---|---|---|---|---|---|---|---|
| | 1 | 2 | 3 | 4 | 5 | 6 | 7 | 8 |
| 0 | 1392 | 690 | 860 | 992 | 1166 | 704 | 595 | 725 |
| 200 | 1422 | 750 | 902 | 1035 | 1120 | 641 | 525 | 782 |
| 400 | 1455 | 818 | 960 | 1100 | 1092 | 595 | 489 | 885 |
| 600 | 1480 | 885 | 1000 | 1142 | 1052 | 548 | 452 | 980 |
| 800 | 1490 | 925 | 1042 | 1192 | 1010 | 500 | 420 | 1022 |
| | +98 | +235 | +182 | +200 | -156 | -204 | -175 | +297 |
| 1600 | 1540 | 1092 | 1180 | 1350 | 850 | 350 | 292 | 1260 |
| Net | +148 | +402 | +320 | +358 | -316 | -354 | -303 | +535 |

| Load Lbs. | Vertical Deflection Inch A | Horizontal Deflection Inch at the Top of End Diaphragm |
|---|---|---|
| 0 | | |
| | 0.005 | 0.00 |
| 200 | | |
| | 0.0015 | 0.0025 |
| 400 | | |
| | 0.0010 | 0.0005 |
| 600 | | |
| | 0.0005 | |
| | 0.008 | 0.0030 |
| 800 | | |
| | 0.006 | |
| 1,600 | | |

## Horizontal Deflections at Edge A-A

| Load Lbs. | Center of the Edge Inches | Quarter Point of the Edge Inches |
|---|---|---|
| 0 | | |
| | 0.142 | 0.100 |
| 800 | | |

# APPENDIX B

## NOTATIONS

## NOTATIONS

| | |
|---|---|
| A | cross sectional area, $ht$ |
| A, B, CC', a, b, c | subscripts used to denote the edges or joints |
| E | modulus of elasticity of plywood, $1.6 \times 10$ psi |
| F | edge forces |
| $f_1$, $f_2$ | longitudinal stresses of the corresponding plates in case I |
| $f_A$, $f_B$ | corrected longitudinal stresses |
| $f_{BC}$, $f_{CB}$, $f_{AB}$, $f_{BA}$, $f_{CC'}$ | longitudinal (out of plane) stresses, acting on the edge (first subscript) of the corresponding plate |
| $h_1$ | width of the plate AB |
| h | width of the plate BC or CC' |
| $I_\parallel$ | moment of inertia when the face grain is parallel to the span |
| $I_\perp$ | moment of inertia when the face grain is perpendicular to the span |
| k | rigidity coefficient ($k = EI/h$) |
| $\ell$ | span of the roof between end diaphragms |
| o | subscript used to denote the middle of a beam or plate |
| p | line load, |

| | |
|---|---|
| Q | plate load |
| t | thickness of plate |
| w | uniformly distributed load in beam theory analysis |
| w' | uniform distributed load in hipped plate theory analysis |
| Z | section modulus of a plate, considered to act as a beam |
| ' | superscripts used to denote the values in case II, for example, $f_1'$, $f_2'$, $f_A'$, $f_B'$, $\delta_1'$, etc. |
| 1, 2, 3 | subscripts used to denote plates: plate AB as 1, BC as 2, and CC' as 3 |
| $\triangle$ | deflection perpendicular to the plate and also $\triangle = \triangle_{bc} + \triangle_{cb}$ |
| $\triangle_{bc}, \triangle_{cb}$ | deflection of the edge (first subscript) perpendicular to the corresponding plates |
| $\triangle_A, \triangle_B$ | deflection perpendicular to the plate AB, at the edges A and B |
| $\triangle_c$ | deflection perpendicular to the plate CC' at the edge C |
| $\delta$ | deflection in the plane of the plate |
| $\delta_{bc}$ | plate deflection of the plate BC, $\delta_{bc} = \delta_{cb}$ |

$\delta_1$          plate deflection of the plate 1 or AB in case I

$\delta_{ab}$         plate deflection of the plate AB, $\delta_{ab} = \delta_1 + \delta_1'$

$\varphi$         angle changes due to the plate rotations